

Figure 3-10. Map showing the location of lysimeters and probes in Focus Area 4.

Table 3-14. Logging completion summary showing depth intervals logged for each Focus Area 4 probe.

| Well_ID | Passive Neutron | | Passive Gamma | | N-gamma | | Moisture | |
|---------|------------------|------------------|------------------|------------------|------------------|------------------|------------------|------------------|
| | Minimum (ft bgs) | Maximum (ft bgs) | Minimum (ft bgs) | Maximum (ft bgs) | Minimum (ft bgs) | Maximum (ft bgs) | Minimum (ft bgs) | Maximum (ft bgs) |
| 741-08C | 4.25 | 21.23 | 4.00 | 21.71 | 3.98 | 20.64 | 0.25 | 21.74 |
| 741-08D | 4.26 | 18.33 | 4.00 | 18.80 | 3.99 | 17.75 | 0.05 | 18.80 |
| 741-10 | 4.24 | 19.20 | 4.00 | 19.67 | 4.00 | 18.56 | 0.25 | 19.69 |
| 741-11 | 4.25 | 19.32 | 4.00 | 19.73 | 4.00 | 18.66 | 0.25 | 19.76 |

Table 3-15. Radionuclide detection summary for Focus Area 4.^a

| Well_ID | Cs-137 662 keV (pCi/g) | Co-60 1,332 keV (pCi/g) | Pu-239 375 keV (pCi/g) | Am-241 662 keV (pCi/g) | Np-237 312 keV (pCi/g) | U-235 186 keV (pCi/g) | U-238 1,001 keV (pCi/g) | Chlorine 1,151 keV (counts/ second) |
|---------|------------------------------|-------------------------------|------------------------------|------------------------------|------------------------------|-----------------------------|-------------------------------|--|
| 741-08C | ND | ND | 462,187.1 | 6,064,204.2 | 56.4 | ND | ND | 6.4 |
| 741-08D | 2.6 | ND | ND | ND | 134.5 | ND | 406.4 | 4.8 |
| 741-10 | ND | ND | ND | ND | ND | 173.1 | 174.6 | 10.5 |

Table 3-15. (continued).

| Well_ID | Cs-137 662 keV (pCi/g) | Co-60 1,332 keV (pCi/g) | Pu-239 375 keV (pCi/g) | Am-241 662 keV (pCi/g) | Np-237 312 keV (pCi/g) | U-235 186 keV (pCi/g) | U-238 1,001 keV (pCi/g) | Chlorine 1,151 keV (counts/ second) |
|------------------|------------------------------|-------------------------------|------------------------------|------------------------------|------------------------------|-----------------------------|-------------------------------|--|
| 741-11 | ND | ND | ND | ND | ND | 12.0 | 74.8 | 6.1 |
| MAX ^b | 140.5 | 814.2 | 194,171,000 | 30,449,000 | 4,881 | 344.9 | 220,894 | 38 |
| PROBE | 741-04 | P9-FI-05 | P9-20 | 743-08-02 | DU-08 | 743-08 | 743-08 | P9-03 |

a. Concentration estimates obtained from geophysical logging measurements can be significantly affected by heterogeneous subsurface conditions; values presented in this table should be viewed as *apparent* concentration.

b. Maximum observed value of radionuclide or element from previous SDA logging.

NA = not applicable
ND = not detected
SDA = Subsurface Disposal Area

3.7.1 Investigation of Plutonium in Lysimeters L1 and L2

Lysimeters L1 and L2 and Type A Probe 741-08 showed evidence for the presence of plutonium. Probes 741-08A and 741-08B, installed between the lysimeters and Probe 741-08, showed no evidence for plutonium, suggesting that the plutonium observed in Probe 741-08 was most likely not the source of plutonium found in the lysimeter samples. Therefore, new probes (i.e., 741-10 and 741-11) were installed on the opposite side of the lysimeters, in the direction of a geophysical anomaly that could indicate the presence of buried drum-waste, to explore for an alternative plutonium source. These probes showed no evidence of plutonium.

The new probes show low-level U-235 and U-238 intervals. Table 3-16 gives the U-235:U-238 activity ratios and mass ratios at each point where both U-235 and U-238 were detected. These ratios have not been corrected for differential gamma ray attenuation, but are suggestive of enriched uranium. In addition to the measurements shown in Table 3-16, 15 additional measurements showed detection of U-235 with no corresponding detection of U-238. Note that low levels of U-235 (and no U-238) were also detected in probes 741-08A and 741-08B.

Table 3-16. Summary of uranium detection in Focus Area 4.^a

| Well_ID | Depth (ft) | U-235 ^a 186-keV (pCi/g) | U-238 1,001-keV (pCi/g) | Activity Ratio ^c U-235:U-238 | Mass Ratio ^c U-235:U-238 |
|---------|---------------|--|-------------------------------|--|--|
| 741-10 | 13.0 | 7.04 | 59.24 | 0.019 | 0.0185 |
| 741-11 | 11.5 | 12.01 | 64.44 | 0.186 | 0.0290 |
| 741-11 | 11.0 | 6.67 | 74.83 | 0.089 | 0.0139 |
| 741-10 | 11.5 | 107.07 | 118.48 | 0.904 | 0.1406 |
| 741-10 | 12.0 | 173.12 | 148.62 | 1.16 | 0.1812 |
| 741-10 | 12.5 | 38.22 | 174.60 | 0.219 | 0.0340 |

a. Concentration estimates obtained from geophysical logging measurements can be significantly affected by heterogeneous subsurface conditions; values presented in this table should be viewed as *apparent* concentration.

b. U-235 apparent concentrations not corrected for potential Ra-226 interference.

c. The following are derived from constants obtained from GE (1989): (1) typical activity ratios: <0.04507 (depleted), 0.04507 (natural), >0.04507 (enriched); (2) typical mass ratios: <0.00696 (depleted), 0.00696 (natural), >0.00696 (enriched)

Moderate chlorine levels and elevated Th-228 also are observed in both probes. The chlorine and thorium intervals coincide with and overlap the uranium interval.

3.7.2 Investigation of Plutonium in Probe 741-08

Azimuthal logging in Probe 741-08 indicated that the plutonium source observed in this probe was located to the east-southeast at 8 ft bgs. This radionuclide zone also contained Am-241 and Np-237. New probes (i.e., 741-08C and 741-08D) were installed in this direction to investigate the extent of plutonium.

Figure 3-11 shows a comparison between probeholes 741-08, 741-08C, and 741-08D. These plots show evidence that the americium-neptunium-plutonium zone in Probe 741-08 extends toward Probe 741-08C, but not toward Probe 741-08D. The radionuclide zone observed in Probe 741-08C has depth and thickness similar to its counterpart in Probe 741-08; however, the apparent Pu-239 and Np-237 concentrations are nearly an order of magnitude lower. The apparent Am-241 concentrations for the two probes are comparable. This circumstance suggests that the plutonium and neptunium are directly associated with each other in the waste form, but are not directly associated with the americium.

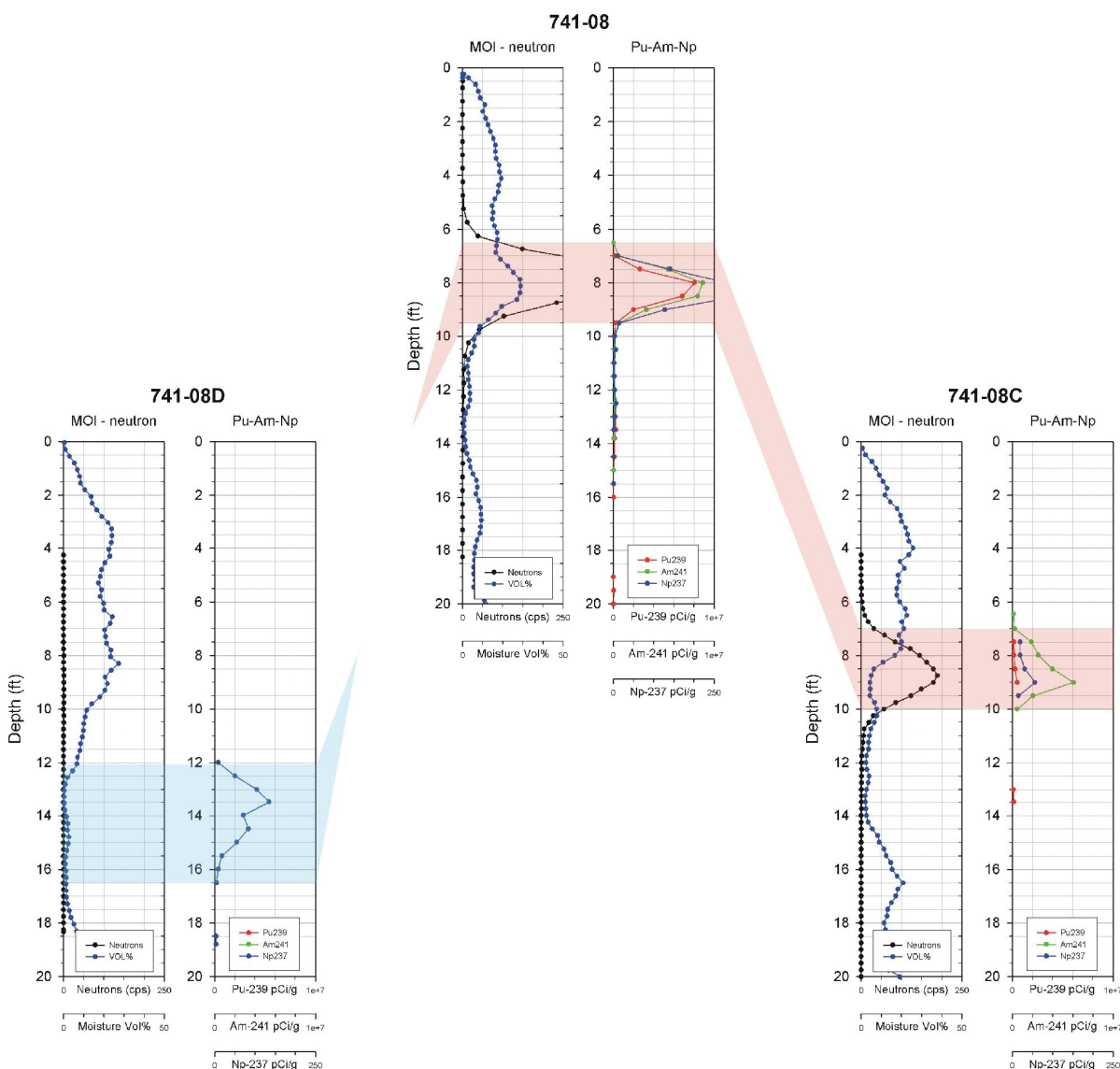


Figure 3-11. Comparison of selected logging results for probeholes 741-08, 741-08C, and 741-08D.

3.8 Focus Area 5: Pit 6 Plutonium Waste from the Rocky Flats Plant

Focus Area 5 targets are RFP drum shipments in Pit 6 suspected to contain plutonium-contaminated waste. Three probes were installed based on the combined evaluation of inventory records and surface geophysics (see Figure 3-12). Probes P6-PU-1 and P6-PU-2 were installed to a depth of 20.0 ft. Probe P6-PU-3 met refusal at 8.0 ft, where it is suspected to have struck impenetrable waste. Moisture data at the bottom of Probe P6-PU-3 suggest a waste zone beginning at 7.5-8.0 ft bgs.

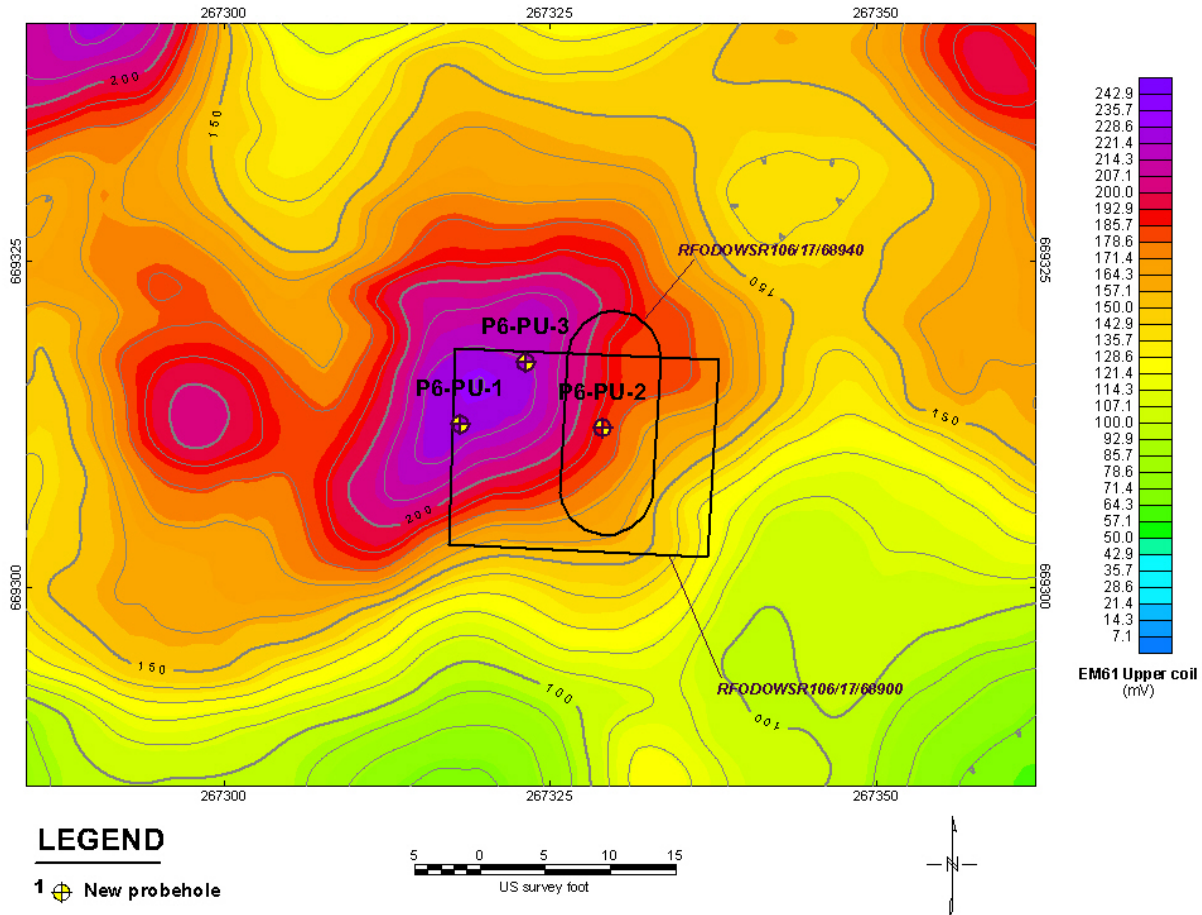


Figure 3-12. Map showing the location of Focus Area 5.

Tables 3-17 and 3-18 present summaries of the logged intervals and the detected contaminants for each Focus Area 5 probe. A logging data summary chart for each Focus Area 5 probe is included in Appendix B. Note that radionuclide levels are presented in units of activity concentration. These values should be understood as *apparent* concentrations, because the actual concentration is highly dependent on heterogeneity in the vicinity of the probehole.

Table 3-17. Logging completion summary showing depth intervals logged for each Focus Area 5 probe.

| Well_ID | Passive Neutron | | Passive Gamma | | N-gamma | | Moisture | |
|---------|---------------------|---------------------|---------------------|---------------------|---------------------|---------------------|---------------------|---------------------|
| | Minimum (ft bgs) | Maximum (ft bgs) | Minimum (ft bgs) | Maximum (ft bgs) | Minimum (ft bgs) | Maximum (ft bgs) | Minimum (ft bgs) | Maximum (ft bgs) |
| P6-PU-1 | 4.25 | 19.59 | 4.00 | 19.92 | 4.00 | 18.82 | 0.25 | 19.92 |
| P6-PU-2 | 4.25 | 19.43 | 4.00 | 20.06 | 4.00 | 19.02 | 0.25 | 20.05 |
| P6-PU-3 | 4.25 | 7.38 | 4.00 | 7.80 | 4.00 | 6.74 | 0.25 | 7.88 |

Table 3-18. Radionuclide detection summary for Focus Area 5.^a

| Well_ID | Cs-137 662 keV (pCi/g) | Co-60 1,332 keV (pCi/g) | Pu-239 375 keV (pCi/g) | Am-241 662 keV (pCi/g) | Np-237 312 keV (pCi/g) | U-235 186 keV (pCi/g) | U-238 1,001 keV (pCi/g) | Chlorine 1,151 keV (counts/ second) |
|------------------|------------------------------|-------------------------------|------------------------------|------------------------------|------------------------------|-----------------------------|-------------------------------|--|
| P6-PU-1 | ND | ND | 7,943,767.1 | 42,117,789.8 | 593.7 | ND | 573.8 | 5.3 |
| P6-PU-2 | ND | ND | 1,590,915.7 | 1,129,598.6 | 12.1 | ND | 28.1 | 2.8 |
| P6-PU-3 | ND | ND | 1,234,124.6 | 551,023.7 | 8.1 | ND | ND | ND |
| MAX ^b | 140.5 | 814.2 | 194,171,000 | 30,449,000 | 4,881 | 344.9 | 220,894 | 38 |
| PROBE | 741-04 | P9-FI-05 | P9-20 | 743-08-02 | DU-08 | 743-08 | 743-08 | P9-03 |

a. Concentration estimates obtained from geophysical logging measurements can be significantly affected by heterogeneous subsurface conditions; values presented in this table should be viewed as *apparent* concentration.

b. Maximum observed value of radionuclide or element from previous SDA logging.

NA = not applicable

ND = not detected

SDA = Subsurface Disposal Area

Probes P6-PU-1 and P6-PU-2 encountered high levels of americium, neptunium, and plutonium. Probe P6-PU-1 log data indicate the highest apparent Am-241 concentration observed anywhere in SDA logging to date. Uranium-238 and chlorine were observed to be sporadically associated with the americium-neptunium-plutonium radionuclide zones.

The apparent presence of a thick soil layer beneath the waste in probes P6-PU-1 and P6-PU-2 offers an opportunity to evaluate the possible migration of radionuclides into the underburden. Therefore, several long-count measurements were conducted in the underburden of these probes. The long-count data show that migration of radionuclides into underburden soils is very limited. Section 4.4 contains a further discussion of long-count data results.

Azimuthal logging was conducted in probeholes P6-PU-1 (seven depths), P6-PU-2 (six depths), and P6-PU-3 (one depth). Azimuthal data are presented in Section 4.5.

3.9 Focus Area 6: Pit 10 Plutonium Waste

Focus Area 6 probe targets are RFP drum shipments in Pit 10 suspected to contain plutonium contaminated waste. Three probes were installed based on combined evaluation of inventory records and surface geophysics (see Figure 3-13). Probes P10-PU-1 and P10-PU-2 met refusal at 5.5 and 10.0 ft respectively. Probe P10-PU-3 was installed to nearly 21.0 ft. These circumstances suggest that probe P10-PU-1 and P10-PU-2 may have struck impenetrable waste.

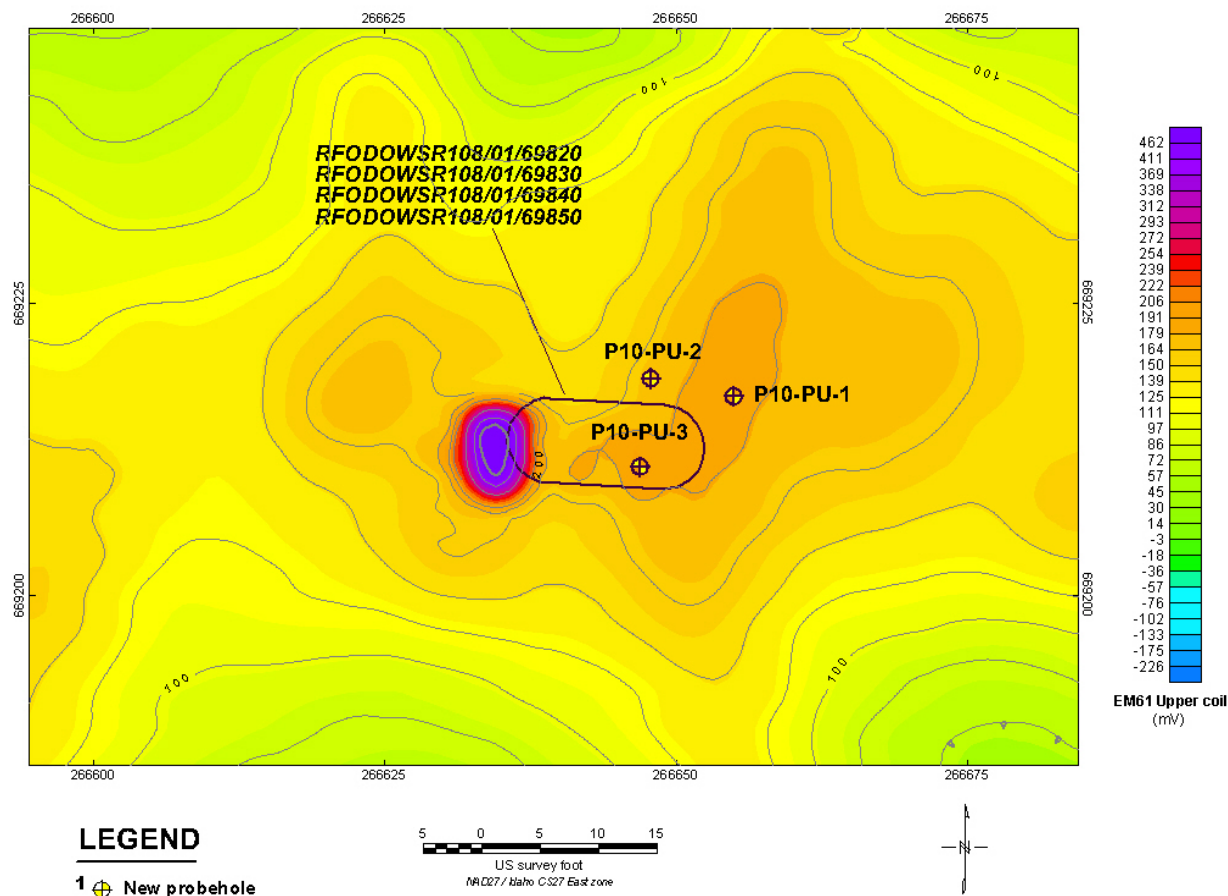


Figure 3-13. Map showing location of Focus Area 6 probes.

Tables 3-19 and 3-20 present summaries of the logged intervals and the detected contaminants for each of the Focus Area 6 probes. A logging data summary chart for each Area 6 probe is included in Appendix B. Note that radionuclide levels are presented in units of activity concentration. These values should be understood as *apparent* concentrations, since the actual concentration is highly dependent on heterogeneity in the vicinity of the probehole.

Table 3-19. Logging completion summary showing depth intervals logged for each Focus Area 6 probe.

| Well_ID | Passive Neutron | | Passive Gamma | | N-gamma | | Moisture | |
|----------|---------------------|---------------------|---------------------|---------------------|---------------------|---------------------|---------------------|---------------------|
| | Minimum (ft bgs) | Maximum (ft bgs) | Minimum (ft bgs) | Maximum (ft bgs) | Minimum (ft bgs) | Maximum (ft bgs) | Minimum (ft bgs) | Maximum (ft bgs) |
| P10-PU-1 | 4.24 | 5.10 | 4.00 | 5.54 | 4.00 | 4.48 | 0.25 | 5.58 |
| P10-PU-2 | 4.24 | 9.60 | 4.00 | 10.07 | 4.00 | 8.97 | 0.25 | 10.10 |
| P10-PU-3 | 4.25 | 19.86 | 4.00 | 20.31 | 4.00 | 19.26 | 0.24 | 20.50 |

Table 3-20. Radionuclide detection summary for Focus Area 6.^a

| Well_ID | Cs-137 662 keV (pCi/g) | Co-60 1,332 keV (pCi/g) | Pu-239 375 keV (pCi/g) | Am-241 662 keV (pCi/g) | Np-237 312 keV (pCi/g) | U-235 186 keV (pCi/g) | U-238 1,001 keV (pCi/g) | Chlorine 1,151 keV (counts/ second) |
|------------------|------------------------------|-------------------------------|------------------------------|------------------------------|------------------------------|-----------------------------|-------------------------------|--|
| P10-PU-1 | ND | ND | ND | ND | ND | ND | ND | 1.3 |
| P10-PU-2 | ND | ND | ND | ND | ND | ND | ND | 14.6 |
| P10-PU-3 | ND | ND | 21,301.0 | ND | ND | ND | ND | 8.7 |
| MAX ^b | 140.5 | 814.2 | 194,171,000 | 30,449,000 | 4,881 | 344.9 | 220,894 | 38 |
| PROBE | 741-04 | P9-FI-05 | P9-20 | 743-08-02 | DU-08 | 743-08 | 743-08 | P9-03 |

a. Concentration estimates obtained from geophysical logging measurements can be significantly affected by heterogeneous subsurface conditions;

values presented in this table should be viewed as *apparent* concentration.

b. Maximum observed value of radionuclide or element from previous SDA logging.

NA = not applicable

ND = not detected

SDA = Subsurface Disposal Area

No man-made radionuclides were detected in any of the Focus Area 6 probes, except for one low-level Pu-239 detection in Probe P10-PU-3. All three probes showed the presence of low-to-moderate levels of chlorine.

3.10 Focus Area 7: Pit 2 Concentrated Rocky Flats Plant Drums

Focus Area 7 targets are plutonium-contaminated graphite molds in Pit 2. Pit 2 inventory records were first evaluated to identify waste shipments that could potentially contain graphite molds. Search criteria were:

- Generator: Building 776
- Waste type: Type 5 (noncombustible)
- Weight: approximately 200 lb.

Figure 3-14 shows two areas found to contain the largest concentration of drums meeting the search criteria, using inventory data. Historical documents indicate that Pit 2 waste drums were carefully stacked in rows rather than randomly dumped as in later SDA disposal operations. The final position of the probes was adjusted to coincide with strong anomalies observed in surface geophysics data. These anomalies were interpreted to show the position of buried drums. Figure 3-14 also shows targeted drum concentrations, surface geophysics (magnetic field data), and the installed position of the six Pit 2 probes.

The probes were installed during December 2003, and the driller observed that the probes did not go in as smoothly as others have in the past. The drilling process experienced numerous stops and starts, suggesting alternating harder and softer zones in the subsurface. The driller also indicated that a screeching sound of metal on metal was heard during each probe installation.

Tables 3-21 and 3-22 present summaries of the logged intervals and the detected contaminants for each of the Focus Area 7 probes. A logging data summary chart for each Focus Area 7 probe is included in Appendix B. Note that radionuclide levels are presented in units of activity concentration. These values should be understood as *apparent* concentrations, because the actual concentration is highly dependent on heterogeneity in the vicinity of the probehole.

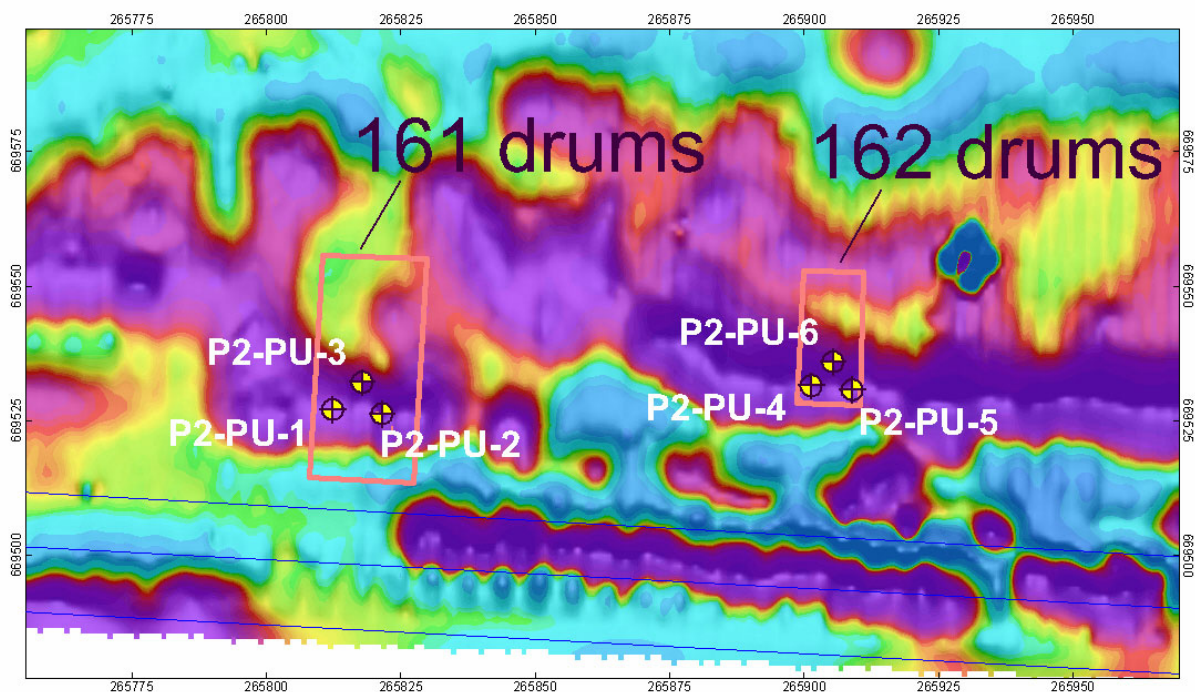


Figure 3-14. Targeted drum concentrations, surface geophysics (magnetic field data), and the installed position of the six Pit 2 probes.

Table 3-21. Logging completion summary for the new Pit 2 probes.

| Well_ID | Passive Neutron | | Passive Gamma | | N-gamma | | Moisture | |
|---------|---------------------|---------------------|---------------------|---------------------|---------------------|---------------------|---------------------|---------------------|
| | Minimum (ft bgs) | Maximum (ft bgs) | Minimum (ft bgs) | Maximum (ft bgs) | Minimum (ft bgs) | Maximum (ft bgs) | Minimum (ft bgs) | Maximum (ft bgs) |
| P2-PU-1 | 9.76 | 18.09 | 2.00 | 18.47 | 2.00 | 17.49 | 0.25 | 18.61 |
| P2-PU-2 | 2.25 | 13.83 | 2.00 | 14.29 | 2.00 | 13.14 | 0.25 | 14.33 |
| P2-PU-3 | 11.25 | 20.14 | 2.00 | 20.52 | 2.00 | 19.46 | 0.25 | 20.59 |
| P2-PU-4 | 4.25 | 12.18 | 2.00 | 12.63 | 2.00 | 11.58 | 0.25 | 12.66 |
| P2-PU-5 | 2.25 | 12.04 | 2.00 | 12.49 | 2.00 | 11.45 | 0.25 | 12.52 |
| P2-PU-6 | 2.25 | 14.62 | 2.00 | 15.11 | 2.00 | 14.00 | 0.25 | 15.13 |

Table 3-22. Radionuclide detection summary for Focus Area 7.^a

| Well_ID | Cs-137 662 keV (pCi/g) | Co-60 1,332 keV (pCi/g) | Pu-239 375 keV (pCi/g) | Am-241 662 keV (pCi/g) | Np-237 312 keV (pCi/g) | U-235 186 keV (pCi/g) | U-238 1,001 keV (pCi/g) | Chlorine 1,151 keV (counts/ second) |
|---------|------------------------------|-------------------------------|------------------------------|------------------------------|------------------------------|-----------------------------|-------------------------------|--|
| P2-PU-1 | ND | ND | 46,366,044.4 | 13,049,853.1 | ND | 6.3 | ND | 3.9 |
| P2-PU-2 | ND | ND | 3,298,986.8 | 3,417,208.1 | ND | ND | ND | 5.7 |
| P2-PU-3 | ND | ND | ND | ND | ND | ND | 2,216.8 | 2.2 |
| P2-PU-4 | ND | ND | 330,830.6 | 120,077.6 | ND | 200.6 | 82,055.1 | 2.3 |
| P2-PU-5 | ND | ND | 2,138,749.9 | 665,430.0 | ND | 78.8 | 21.8 | 13.6 |
| P2-PU-6 | ND | ND | 2,046,223.8 | 607,892.8 | ND | 330.1 | 482.2 | 6.7 |

Table 3-22. (continued).

| Well ID | Cs-137 662 keV (pCi/g) | Co-60 1,332 keV (pCi/g) | Pu-239 375 keV (pCi/g) | Am-241 662 keV (pCi/g) | Np-237 312 keV (pCi/g) | U-235 186 keV (pCi/g) | U-238 1,001 keV (pCi/g) | Chlorine 1,151 keV (counts/ second) |
|------------------|------------------------------|-------------------------------|------------------------------|------------------------------|------------------------------|-----------------------------|-------------------------------|--|
| MAX ^a | 140.5 | 814.2 | 194,171,000 | 30,449,000 | 4,881 | 344.9 | 220,894 | 38 |
| PROBE | 741-04 | P9-FI-05 | P9-20 | 743-08-02 | DU-08 | 743-08 | 743-08 | P9-03 |

a. Concentration estimates obtained from geophysical logging measurements can be significantly affected by heterogeneous subsurface conditions; values presented in this table should be viewed as *apparent* concentration.

b. Maximum observed value of radionuclide or element from previous SDA logging.

NA = not applicable

ND = not detected

SDA = Subsurface Disposal Area

Moisture logs for these six probes show a dramatic decrease in soil moisture at depths from 3.5–7 ft bgs. The sudden decrease in the moisture log is believed to mark the transition from soil overburden into the underlying solid waste. Pit 2 moisture logs are somewhat unique in that the moisture log reading drops very nearly to zero and sustains near-zero readings over significant depth intervals. Probe P2-PU-3 exhibits the single exception to this pattern. This moisture log characteristic suggests a thick consistent waste zone that may exist because the drums are stacked, and little or no soil is between the stacked drums. Moisture curves for probes P2-PU-4, P2-PU-5, and P2-PU-6 also show a steep increase in overburden soil moisture content that reaches 50%, which may be due to the geomembrane on the surface. The base of the waste zone varies from 12.4–14 ft bgs.

Logging data show that Pit 2 probes penetrated zones with significant plutonium and americium. The measured plutonium levels in Probe P2-PU-1 are among the highest observed anywhere in the SDA. (Note that only probes P9-20, 743-12, and DU-15 showed higher apparent plutonium levels.) The zones with plutonium and americium occupy only a portion of the waste intervals (i.e., significant portions of the waste zones show no man-made radionuclides). Zones contaminated with U-235 and/or U-238 are observed in four of the six probes. Levels of U-238 in Probe P2-PU-4 are among the highest observed anywhere in the SDA. Ratios of U-235:U-238 in probes P2-PU-3 and P2-PU-4 suggest depleted uranium, and the ratios in P2-PU-5 and P2-PU-6 suggest enriched uranium (see Table 3-22). The zones containing uranium generally occur at distinctly different depths than the zones containing americium and plutonium. Also, some of the radionuclide zones occur in discrete 2-ft intervals, which are interpreted to correspond with individual drums.

Chlorine is prevalent throughout the waste layer, as is the case shown by most SDA probes that have been logged to date. Chlorine levels are moderate to low compared with results from other SDA probes.

Probes P2-PU-1, P2-PU-2, P2-PU-3, and P2-PU-5 show anomalously high levels of natural uranium.^a Probes P2-PU-3 and P2-PU-4 show anomalously high levels of natural thorium. Dr. C. Koizumi of Stoller observed and discussed these anomalous peaks (see Appendix C) for probe P2-PU-3. He concludes that the thorium anomaly almost certainly points to Th-228 enrichment. One possible mechanism is alpha decay of U-232, but this could not be verified. Dr Koizumi suggests that the apparent excess of natural uranium is consistent with uranium mill tailings or concentrated radium. Neither possibility could be readily verified (see Appendix C).

a. Natural uranium is identified based on 1,764 keV gamma rays from the uranium daughter, Bi-214; man-made uranium is identified based on the 1,001 keV gamma rays emitted by the uranium daughter, Pa-234m.

4. OTHER ANALYSES

4.1 Evaluation of Logging Tool Calibration

During FY 2004, the probing project evaluated the calibration methodology used for converting Type A nuclear logging measurements into quantitative estimates of radionuclide concentration. This section provides a brief synopsis of that evaluation. For more details, refer to the complete report entitled *Evaluation of Nuclear Logging Tool Calibrations for Use in Type A Probes at the Idaho National Engineering and Environmental Laboratory Subsurface Disposal Area* (Giles, Josten, and Broomfield 2003).

4.1.1 Report Summary

This section explores the usefulness of recalibrating logging tools used during Type A probing investigations conducted within the SDA. In particular, limitations of the existing method of calibrating passive gamma ray tools are examined in detail to assess the cause of uncertainty in quantitative results.

The response of the passive gamma ray tool is known to depend on many factors, but the three most important are (1) the amount of radionuclide source present, (2) geometry of the radionuclide source distribution (i.e., anywhere between a compact point source and a homogenous distribution), and (3) density of the waste and soil matrix surrounding the source. Modeling exercises show that these three factors have roughly equal influence on the logging-tool response. As a consequence, the logging data cannot provide an unequivocal estimate for one factor unless the other factors are known. The existing calibration method handles this problem by making simplifying assumptions for the source geometry and soil-matrix density such that the third factor, the amount of radionuclide, can be estimated directly.

Radionuclide estimates produced by the existing calibration methodology have very limited utility because the underlying uniformity assumptions are indefensible. Inventory records, waste drum scan records, and logging data all indicate highly heterogeneous conditions within SDA waste. Furthermore, no known methods will independently measure the waste and soil matrix density. This section considers alternative methods for gamma ray tool calibration and data processing that acknowledge these limitations.

The proposed method would permit some non-TRU areas^b to be directly identified from logging data, which may have some utility for remedial decision-making. However, this information could only be achieved at a very high monetary cost for probe installation, downhole logging, and data processing. The method is conservative by design, and therefore, would produce a large number of false-positive errors where non-TRU areas are incorrectly classified as TRU waste. Furthermore, no allowance is made for exotic conditions that could cause false-negative errors where TRU waste is incorrectly classified as non-TRU.

Finally, alternative radiation measurement technologies were investigated to determine their applicability for differentiating TRU waste. Several large-area, long-count-time detectors were considered for deployment on the SDA ground surface. As a class, these tools were found to have no utility at the SDA because of the limited penetration of alpha particles, gamma rays, and neutrons through soil. Emerging-technology radiation-logging tools may significantly improve sensitivity to radionuclides, thus allowing for much faster field operations. However, the new tools will suffer from the same ambiguity

b. Transuranic areas are defined as areas having greater than or equal to 100 nCi/g combined activity from all man-made alpha-emitting radionuclides with a mass number greater than 235 and half lives greater than 20 years.

issues that affect existing logging tools (i.e., uncertainties about source geometry and density of the soil and waste matrix).

4.2 Comparison of Moisture Sampling and Logging Data

4.2.1 Report Conclusions and Recommendations

Because of heterogeneous conditions in the SDA subsurface, most, if not all, Type A probeholes violate the spectral gamma ray logging tool calibration conditions that assume homogenous radionuclide distribution and homogenous waste and soil matrix density. Recalibration of the spectral gamma ray tool to a new standard condition is not recommended because no meaningful standard exists for radionuclide distribution or waste and soil matrix density. Furthermore, information concerning radionuclide distribution and waste and soil matrix density cannot be obtained by any known independent measurement method. Consequently, the spectral gamma ray measurements cannot be meaningfully corrected for heterogeneity.

An alternative approach to calibration and processing of Type A logging data was developed with the sole purpose of screening the subsurface for non-TRU waste. To implement this method, a set of standard conditions is defined under which a subsurface volume surrounded by probes may be categorized as either non-TRU or possible-TRU. Possible-TRU areas are subjected to additional processing steps by which some may be recategorized as non-TRU.

By the proposed method, subdivision of the entire SDA into non-TRU and possible-TRU subvolumes can be achieved. However, the method requires the installation, logging, and analysis of approximately 15,600 Type A probes per acre. Furthermore, both false-positive errors (non-TRU waste categorized as possible-TRU) and false-negative errors (TRU waste categorized as non-TRU) are possible. The proportion of the two error types depends on the choice of standard conditions. For example, if standard conditions are chosen conservatively, many false-negatives may be avoided, but a large number of false-positives will be generated.

Alternative radiation measurement technologies were investigated to determine their applicability for differentiating TRU waste. Several large-area, long-count-time detectors were considered for deployment on the SDA ground surface. As a class, these tools were found to have no utility at the SDA because of the limited penetration of alpha particles, gamma rays, and neutrons through soil. New emerging radiation logging tools may be very useful for TRU differentiation if employed in a high probe-density survey as described in the Giles, Josten, and Broomfield (2003) report. The primary benefit of these tools will be improved speed of operation. As proposed, the new tools implement more sophisticated data acquisition and processing schemes and may, therefore, produce more detailed radionuclide and elemental information that would provide additional constraints on three-dimensional modeling. However, these tools will not significantly improve the ability to directly identify non-TRU waste, because they will suffer from the same uncertainties about source geometry and density of the soil and waste matrix.

Despite the difficulties (improbabilities) associated with calibrating the tools for quantitative purposes, the existing data set and any logging data gathered in the future may be used qualitatively in identifying waste types, and waste zone composition, and in providing information directing quantitative investigations.

4.3 Comparison of Moisture Sampling and Logging Data in Focus Area 3

New neutron-neutron moisture logging data for Focus Area 3 were obtained in the shallow vadose zone (i.e., less than 20 ft) of the SDA during August and September 2003. The Type A neutron-neutron logging tool reports moisture content in excess of 30 volume percent (vol%) for Focus Area 3 probes P5-UEU-1, P5-UEU-3, P5-UEU-4, P5-UEU-5, P5-UEU-6, and P5-UEU-8. These moisture-content readings occur within the first few feet of the subsurface, despite the excessively dry summer conditions and long-term drought that has affected southeast Idaho. The readings are also anomalously high compared with other SDA probes including nearby probes in Pit 5 (see Figures 4-1 and 4-2).

4.3.1 Density Effect on Moisture Logging Data

The logging subcontractor made no density correction to the moisture data. However, their vendor data submittals discuss the density effect on moisture logging. In general, if the density of the formation is greater than the calibration density, the actual moisture vol% is less than the measured value. Moisture data for Focus Area 3 exhibits the opposite case (i.e., anomalously high moisture contents). Soil density in the UEU-probe area would have to be anomalously low for density effects to have produced anomalously high moisture contents. This seems implausible, because the probes in questions are located on a roadway and have been compacted by vehicle traffic over many years. Furthermore, it is physically impossible that densities could be low enough to change apparent moisture content by 10 vol% or more. Therefore, it is unlikely that the observed high moisture contents in the UEU probes are caused by density effects.

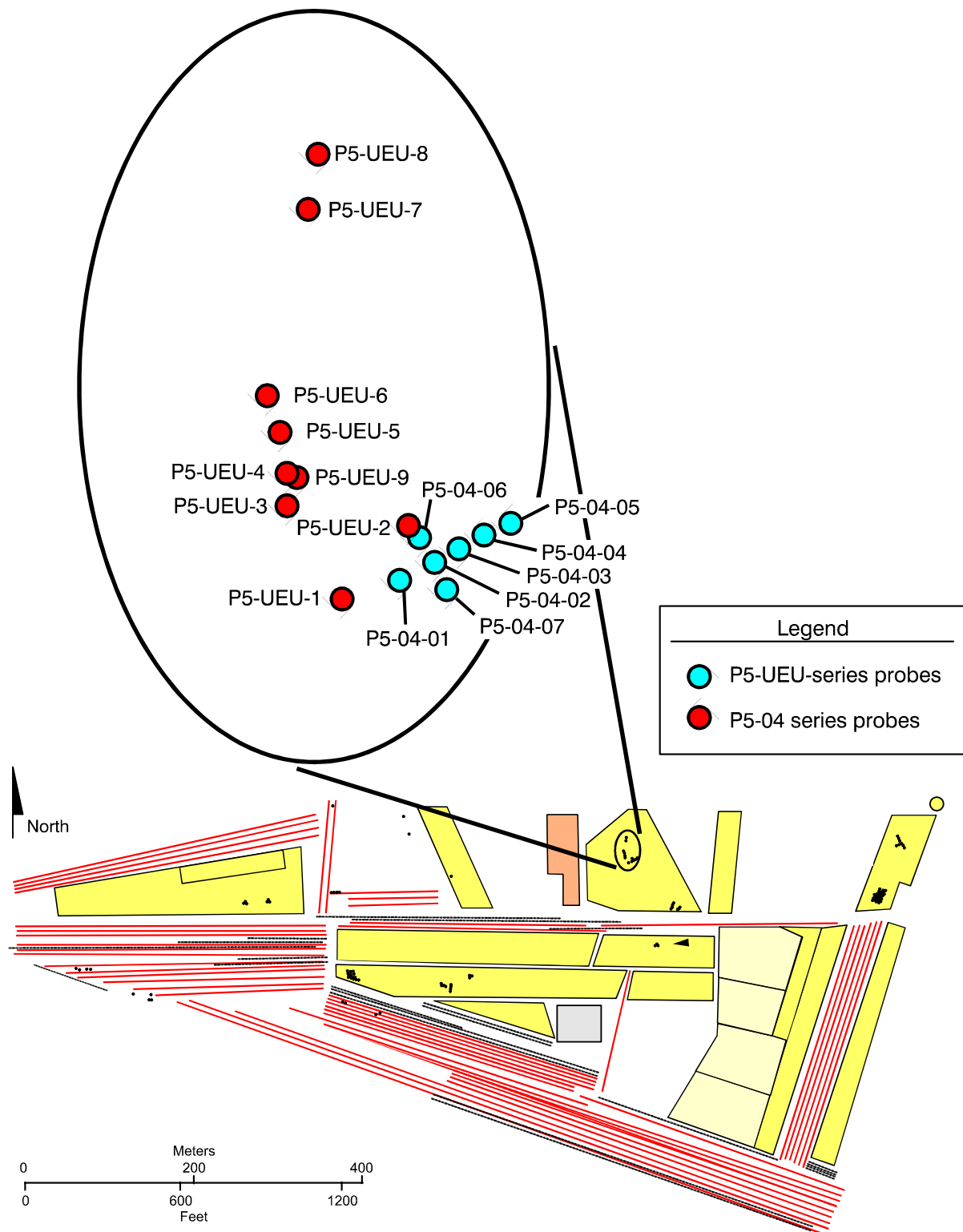
4.3.2 Field Verification of the Moisture Tool Calibration

The moisture logging tool that produced the new data was calibrated at Hanford by the logging subcontractor; however, no field results check had ever been performed. For this reason, a small soil-sampling effort was initiated to provide an independent evaluation of the tool performance and calibration.

Three locations were selected for soil sampling adjacent to Type A probes, HAL1, UD-01, and P5-UEU-4, representing low, medium, and high soil moisture respectively. Soil samples were collected within 6 in. of the probe locations, on the southwest side of the probe, at depths of 1.0, 2.0, and 3.0 ft bgs. Samples were analyzed on a gravimetric basis, using ASTM D2216-98, "Standard Test Method for Laboratory Determination of Water (Moisture) Content of Soil and Rock by Mass."

Soil-sampling results in weight percent (wt%) are listed in Table 4-1, along with a computed value for the corresponding vol% to facilitate comparison with moisture-logging data. The conversion between wt% and vol% depends on the soil dry-bulk density, which was taken as 1.44 g/cc based on previous SDA soil sample data (McElroy and Hubbell 1990).

Figure 4-3 compares the soil-sample results with the moisture logging data for each probe. In general, the agreement between the two methods is good. Both data sets show the same trend of low, medium, and high soil moisture for the three probes. Small discrepancies occur at specific measurement points, but these may be attributed to various factors such as density variation, sampling location, or sampling effects. Overall, the sampling results validate the performance and calibration of the moisture logging tool. Additional information concerning the soil moisture-sampling program is provided in Appendix E.



G1414-02

Figure 4-1. Sketch map showing location of Pit 5 P5-UEU-series and P5-04-series Type A probes.

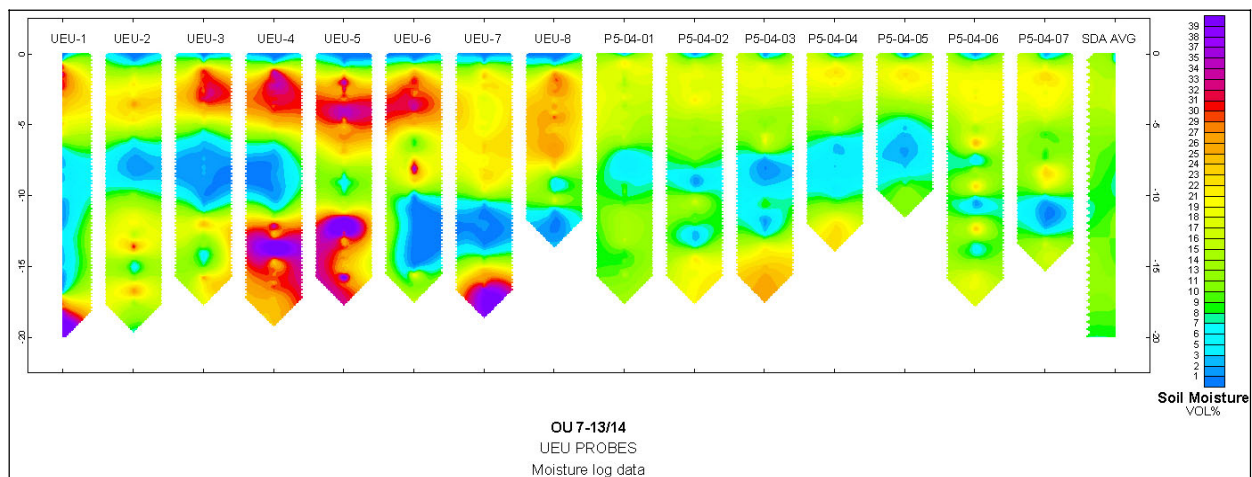


Figure 4-2. Diagram showing the depth variation of neutron-neutron soil moisture readings for the Pit 5 UEU-series and P5-04-series Type A probes.

Table 4-1. Summary of sampling and logging results. Sample volume percent values calculated assuming soil dry-bulk density of 1.44 g/cc.

| Well ID | Sample ID | Depth | Wt% | Vol% ^a | Log Vol% |
|----------|------------|-------|------|-------------------|----------|
| P5-UEU-4 | SMV00601M7 | 1 | 19.5 | 28.1 | 19.2 |
| P5-UEU-4 | SMV00701M7 | 2 | 22.2 | 32.0 | 32.2 |
| P5-UEU-4 | SMV00801M7 | 3 | 24.5 | 35.3 | 32.0 |
| UD-01 | SMV00301M7 | 1 | 13.4 | 19.3 | 16.2 |
| UD-01 | SMV00401M7 | 2 | 16.6 | 23.9 | 22.2 |
| UD-01 | SMV00501M7 | 3 | 19.3 | 27.8 | 22.3 |
| HAL1 | SMV00001M7 | 1 | 8.4 | 12.1 | 7.0 |
| HAL1 | SMV00101M7 | 2 | 7.9 | 11.4 | 8.5 |
| HAL1 | SMV00201M7 | 3 | 6.8 | 9.8 | 11.5 |

a. Volume percent based on a dry bulk density of 1.4 g/cc (McElroy and Hubbell 1990).

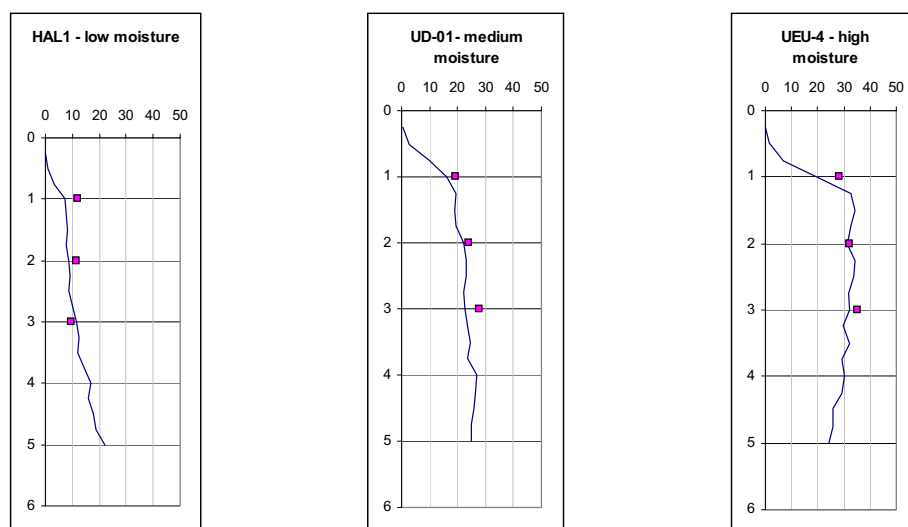


Figure 4-3. Comparison of neutron-neutron moisture logs (curves) and soil moisture sampling results (square point data for three depth locations for each of three probes). Sampling data were converted from weight percent to volume percent based on an assumed dry bulk density of 1.44 g/cc.

4.4 Results from the Long-count Gamma Ray Study

Four 3,000-second long-count spectral gamma ray measurements were performed during December 2003: two in Probehole P6-PU-1 and two in Probehole P6-PU-2. Ten 8-hour long-count measurements were performed in January 2004: five in Probehole P6-PU-1 and five in Probehole P6-PU-2. Measurements were performed within underburden soils beneath the waste zone. The purpose of the long-count measurements was to detect low-level radionuclides, which would indicate the downward migration of radionuclides from the waste zone into the soil. A comparison of the theoretical detection limits for these count times is given in Table 4-2.

Table 4-2. Comparison of theoretical detection limits for count times.

| Radionuclide | Energy (keV) | Detection Limit at 300 Seconds ^a (pCi/g) | Detection Limit at 3,000 Seconds ^b (pCi/g) | Detection Limit at 8 Hours ^b (pCi/g) |
|--------------|-----------------|---|---|---|
| Np-237 | 312 | 1 | 0.32 | 0.10 |
| Pu-239 | 375 | 25,000 | 7,906 | 2,552 |
| Am-241 | 662 | 43,000 | 13,598 | 4,389 |
| Am-241 | 722 | 90,000 | 28,460 | 9,186 |
| U-238 | 1,001 | 10 | 3.16 | 1.02 |

a. Based on minimum detection levels calculated for low-level radionuclide zones in Probehole P6-PU-1.

b. Scaled based on square root of count time.

4.4.1 Three-thousand-second Long-count Results

Figure 4-4a shows a detail of the depth range from 12–16 ft in Probehole P6-PU-1. The waste and soil interface is interpreted to occur at about 14 ft. Two 3,000-second measurements were conducted in soil just below the bottom of waste at 14.5 and 15.5 ft. Plutonium-239, Np-237, and U-238 were detected at 14.5 ft, but were not detected at 15.5 ft. Americium-241 was detected at both 14.5 ft and 15.5 ft, but the Am-241 apparent concentration decreases to just above the 3,000-second detection limit at 15.5 ft. These results suggest that contaminant migration into soils beneath the waste zone is extremely limited.

Figure 4-4b shows a detail of the waste and soil interface in Probehole P6-PU-2. The waste and soil interface is interpreted to occur near 14.5 ft. Low levels of Am-241, Pu-239, and U-238 were detected at 15.0 ft. No radionuclides were detected at 16.0 ft. As for Probehole P6-PU-1, these data suggest that contaminant migration into underburden soils is very limited.

Appendix D contains the subcontractor report describing data processing for the 3,000-second long-count measurements. Plots showing the long-count data are included in Appendix B.

4.4.2 Eight-hour Long-count Results

Five 8-hour long-count measurements were performed in Probehole P6-PU-2 (i.e., at depths of 14.5, 15.0, 15.5, 16.0, 20.06 ft), and five 8-hour long-count measurements were performed in Probehole P6-PU-1 (i.e., at depths of 14.5, 15.0, 15.5, 16.0, and 19.92 ft). The 8-hour long-count data support the conclusions determined from the 3,000-second data (i.e., that contaminant migration into underburden soils is very limited).

Appendix D contains the subcontractor report describing data processing for the 8-hour long-count measurements. Plots showing the long-count data are included in Appendix B.

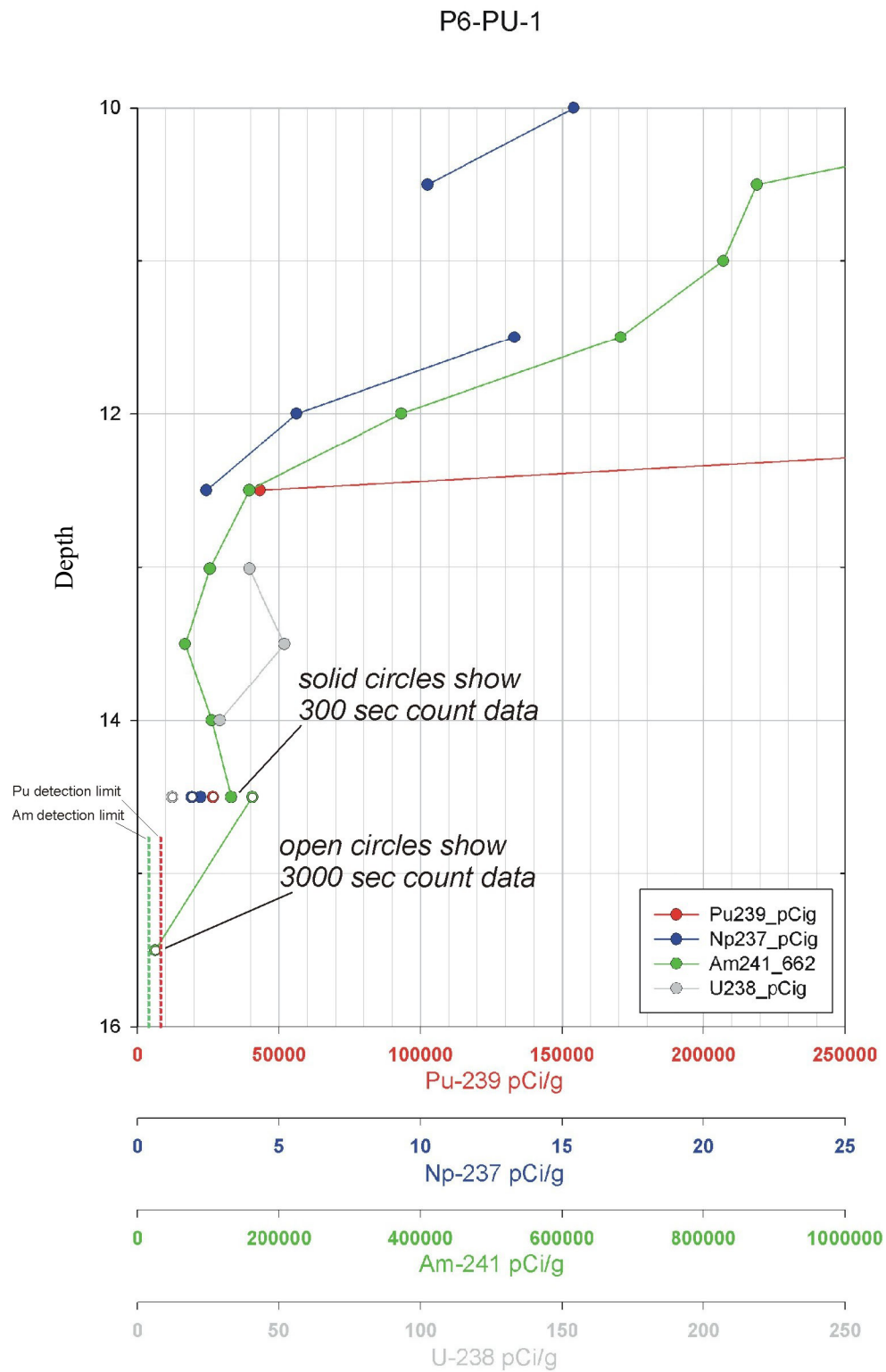


Figure 4-4a. Detail of the depth range from 12–16 ft in Probefhole P6-PU-1.

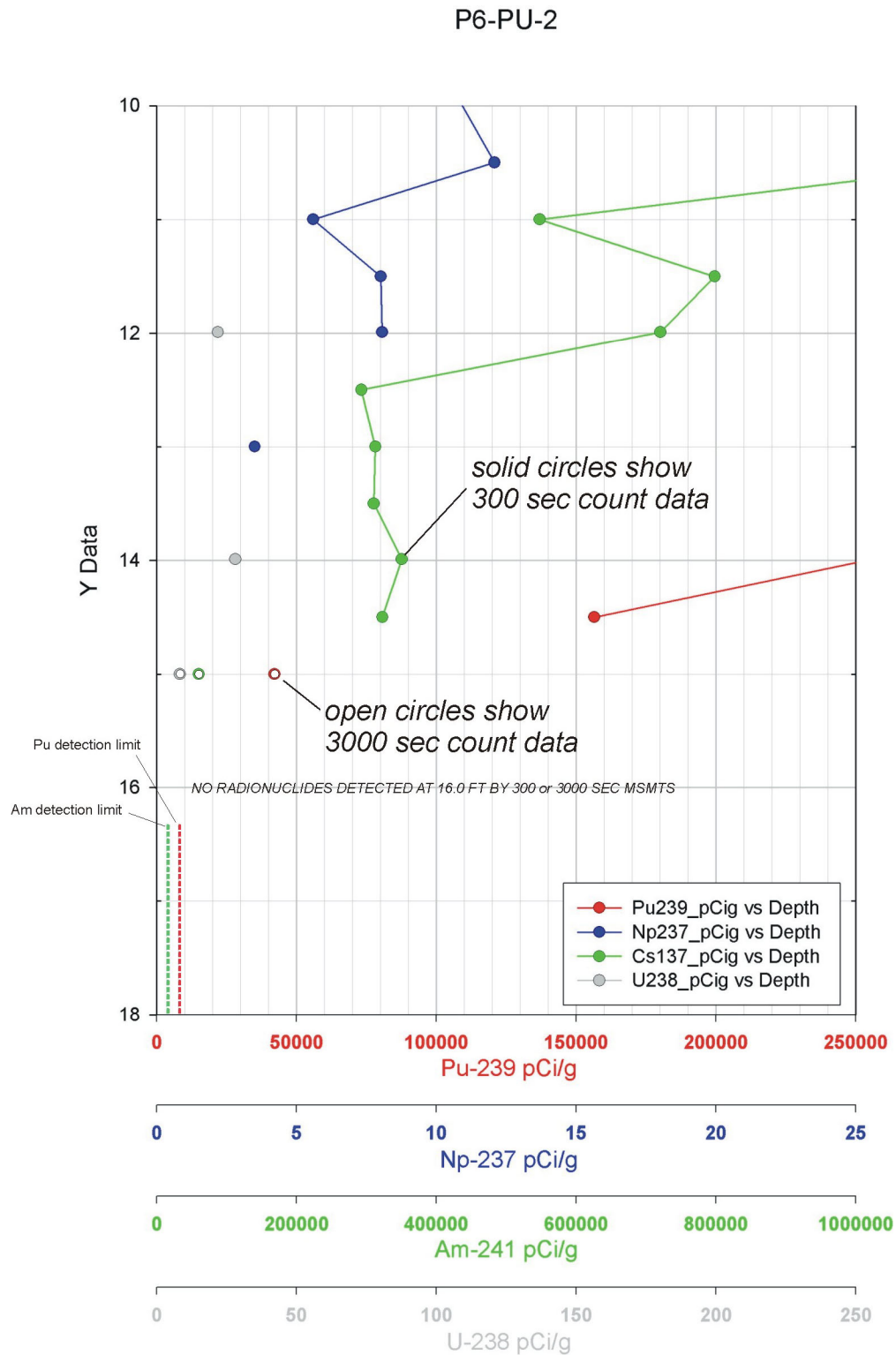


Figure 4-4b. Detail of the waste and soil interface in Probehole P6-PU-2.

4.5 Logging Data Analysis to Support Replacement Tensiometers

Several of the in situ tensiometers installed to investigate SDA subsurface radionuclide areas failed to produce useful data. It was believed that the tensiometers failed because of inadequate coupling with the surrounding media, possibly because the tensiometers were emplaced within solid waste rather than soil. Type A logging data were evaluated to choose locations for replacement tensiometers. Type A data were used to identify subsurface regions likely to contain soil rather than waste.

The original tensiometers that required replacement are listed in Table 4-3 along with the recommended locations for new tensiometers. Figures 4-5–4-9 show cross-section sketches compiled from Type A logging data in the vicinity of these locations.

Table 4-3. Tensiometers requiring replacement and recommended locations for new tensiometers.

| Type A Probe | Tensiometer Number | Depth (ft bgs) | Recommended Location for Replacement Tensiometer | Figure Showing Area |
|--------------|--------------------|----------------|--|---------------------|
| DU-08 | 265 | 6.14 | Between probes DU-08A and DU-08B and as close to Probe DU-08A as practical. | 4-5 |
| DU-08 | 269 | 11.50 | Between probes DU-08A and DU-08B and as close to Probe DU-08A as practical. | 4-5 |
| DU-08 | 270 | 17.86 | Between probes DU-08A and DU-08B and as close to Probe U-08A as practical. | 4-5 |
| DU-10 | 271 | 6.64 | Between probes DU-10A and DU-10B, as close to Probe DU-10A as practical, and in the depth range from 4–6 ft bgs. | 4-6 |
| DU-14 | 278 | 9.83 | No clear soil zones to target. Recommend attempt to emplace tensiometer in thin stringer as indicated in Figure 4-7. Install as close as possible to Probe DU-14A. | 4-7 |
| 743-03 | 226 | 12.31 | At depths and locations shown in Figure 4-8. Install as close as possible to the adjacent Type A probes. | 4-8 |
| 743-03 | 237 | 19.09 | At depths and locations shown in Figure 4-8. Install as close as possible to the adjacent Type A probes. | 4-8 |
| 743-18 | 248 | 12.83 | At depths and locations shown in Figure 4-9. Do not install toward Probe 743-20, because conditions change significantly in this direction. | 4-9 |
| 743-18 | 236 | 19.00 | At depths and locations shown in Figure 4-9. Do not install toward Probe 743-20, because conditions change significantly in this direction. | 4-9 |

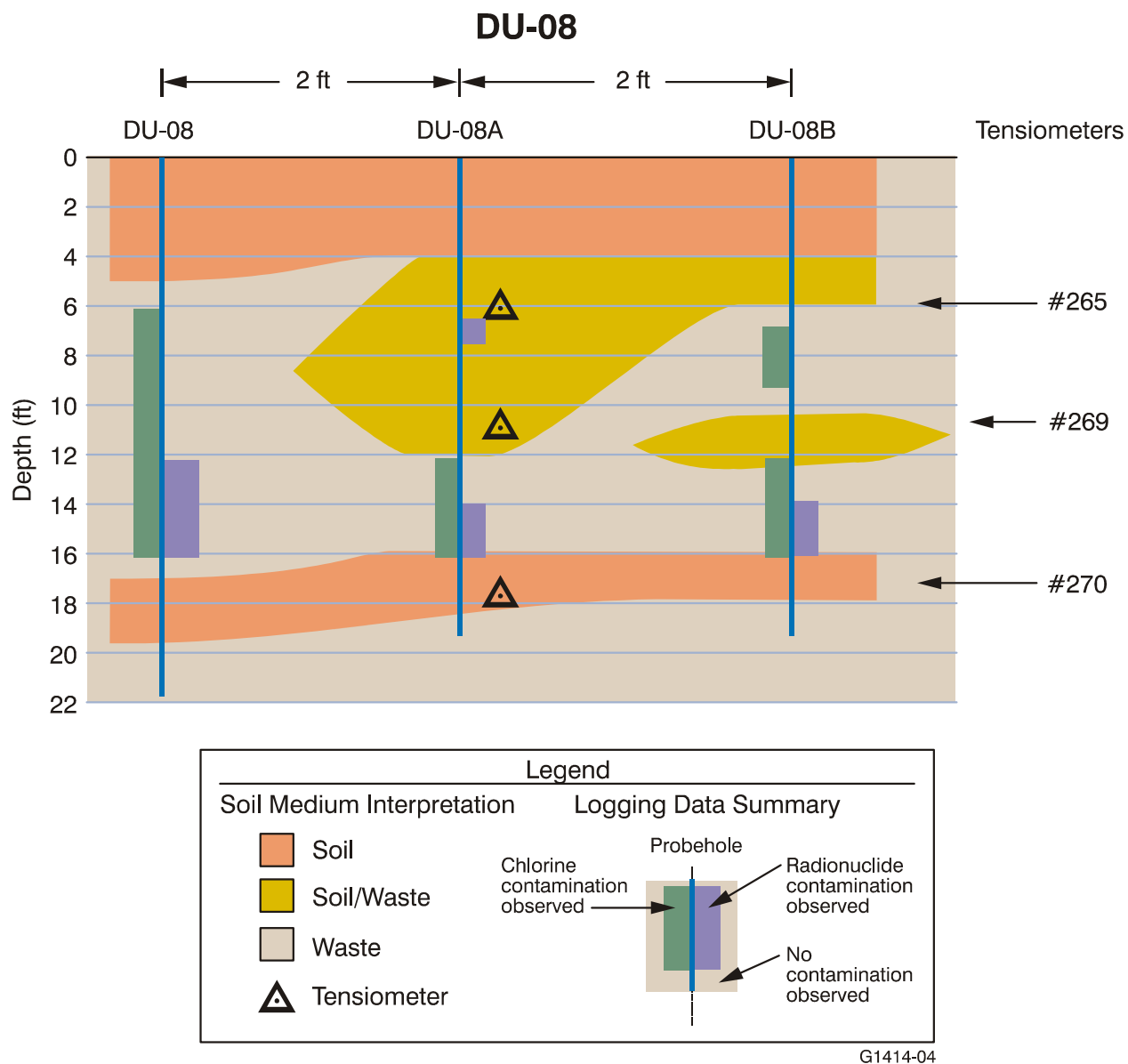
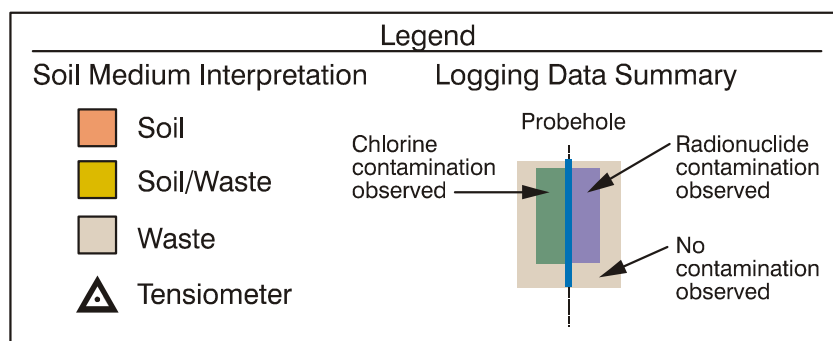
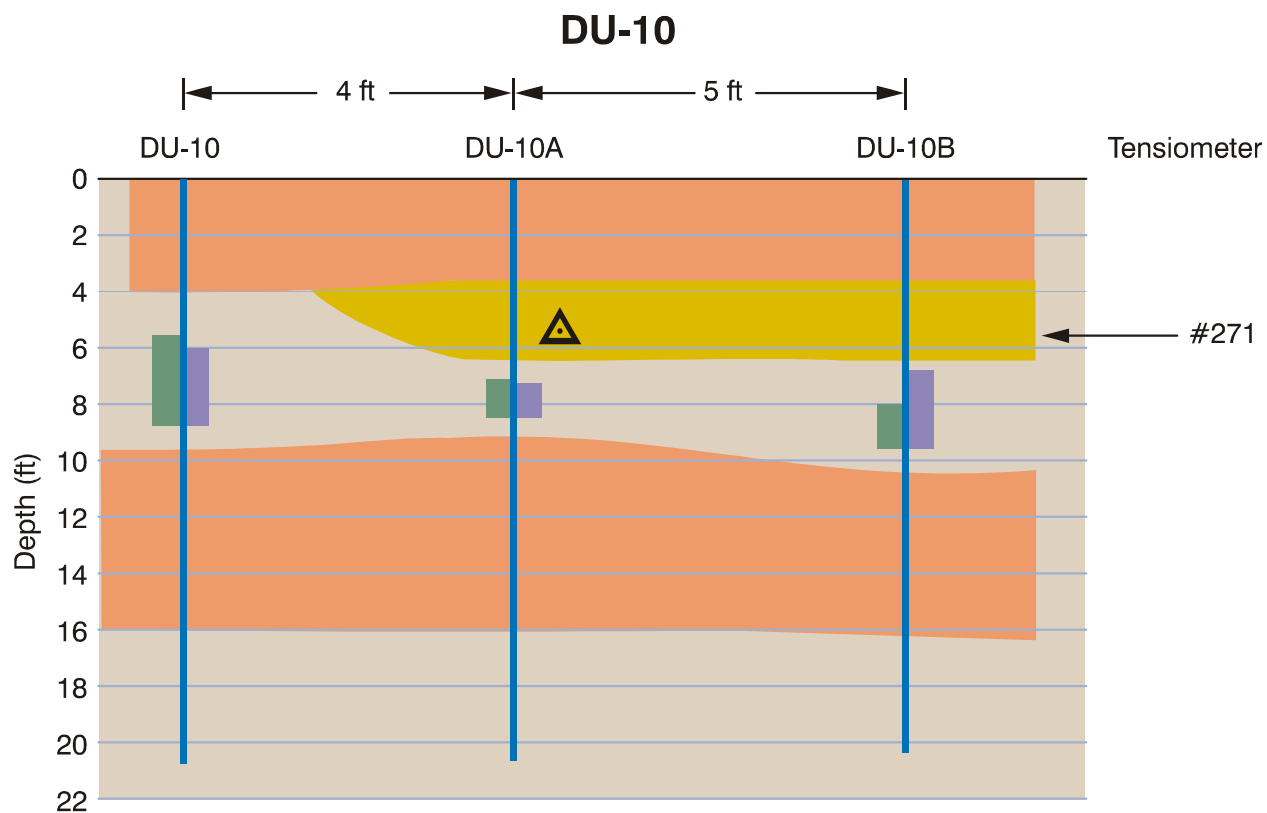


Figure 4-5. Cross-section sketches compiled from Type A logging data near Probe DU-08.



G1414-05

Figure 4-6. Cross-section sketches compiled from Type A logging data near Probe DU-10.

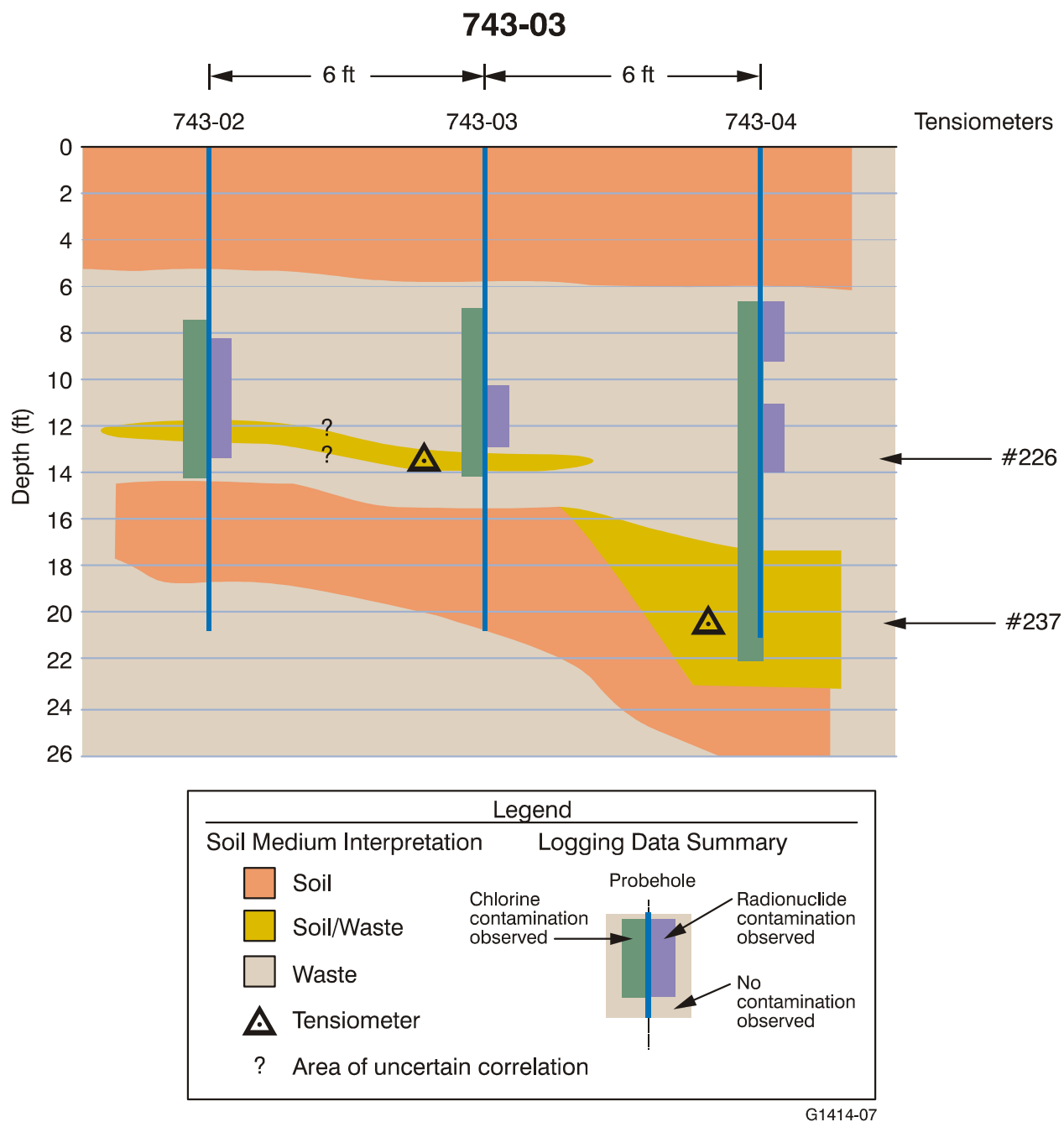


Figure 4-8. Cross-section sketches compiled from Type A logging data near Probe 743-03.

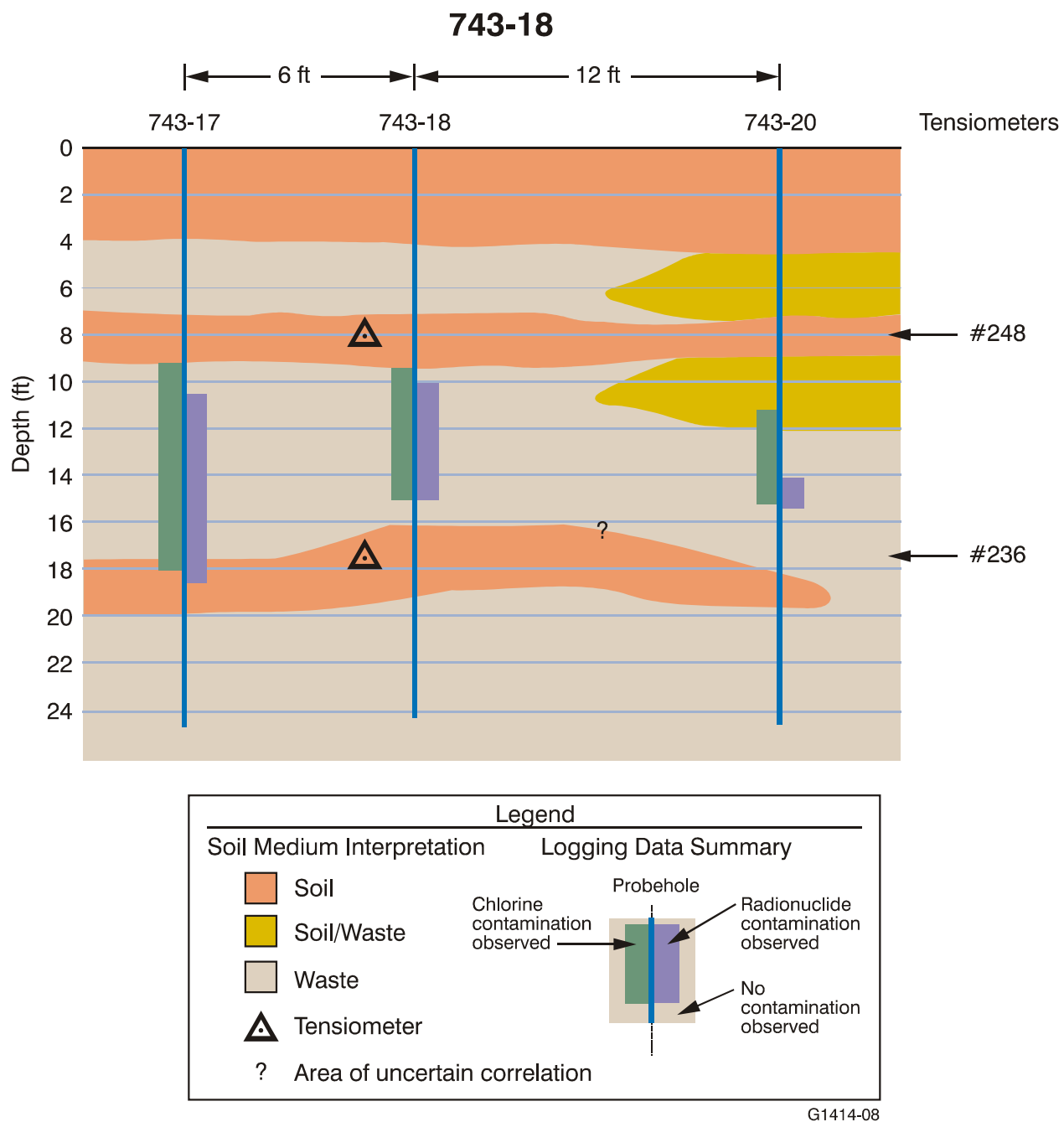


Figure 4-9. Cross-section sketches compiled from Type A logging data near Probe 743-18.

4.6 Analysis of Azimuthal Logging Data

Azimuthal logging was conducted in 13 probes during November–December 2003 (see Table 4-4). Azimuthal logging is conducted with a hyper-pure germanium gamma ray detector contained within a slotted shield. During logging, the tool (and the slot) are rotated through 360 degrees of azimuth, and a gamma ray spectrum is acquired at 22.5-degree increments. The purpose of azimuthal logging is to detect heterogeneous radionuclide distributions as indicated by variation in gamma ray flux with azimuthal direction. Logging depth is held constant during the azimuthal survey. In some cases, azimuthal surveys were conducted at multiple depths in a probehole. A total of 57 azimuthal surveys were conducted during the November–December 2003 logging effort.

Table 4-4. Azimuthal logging data acquisition summary (November–December 2003).

| Focus Area | Pit or Trench | Target | Probe_ID | Depths Logged (ft bgs) |
|------------|---------------|--------------------------|----------|--|
| 1A | Trench 3 | Enriched uranium | T3-EU-02 | 8.0 |
| 1A | Trench 3 | Enriched uranium | T3-EU-03 | 8.0 |
| 1B | Trench 47 | Irradiated fuel | T47-IF-1 | 8.0 |
| 1B | Trench 47 | Irradiated fuel | T47-IF-2 | 8.0, 10.0 |
| 2 | Trench 24 | Liquid waste | HAL2 | 12.0, 21.0 |
| 2 | Trench 24 | Liquid waste | HAL4 | 12.0 |
| 3 | Pit 5 | Uranium/enriched uranium | P5-UEU-1 | 8.0, 8.5, 9.0, 9.5, 10.0, 10.5, 11.0, 11.5, 12.0, 12.5, 13.0, 13.5, 14.0, 14.5, 15.0, 15.5, 16.0 |
| 3 | Pit 5 | Uranium/enriched uranium | P5-UEU-4 | 6.0, 7.0, 8.0, 9.0, 9.5, 10.0, 11.0, 12.0, 13.0, 14.0 |
| 3 | Pit 5 | Uranium/enriched uranium | P5-UEU-5 | 11.0, 12.0, 13.0 |
| 3 | Pit 5 | Uranium/enriched uranium | P5-UEU-7 | 10.0, 11.0, 12.0, 13.0, 14.0 |
| 5 | Pit 6 | Plutonium waste | P6-PU-1 | 6.0, 7.0, 8.0, 9.0, 10.0, 11.0, 12.0 |
| 5 | Pit 6 | Plutonium waste | P6-PU-2 | 9.0, 10.0, 11.0, 12.0, 13.0, 14.0 |
| 5 | Pit 6 | Plutonium waste | P6-PU-3 | 7.74 |

Azimuthal logging results are presented as polar plots that show the variation in gamma ray flux with azimuthal direction (see Appendix B). Two examples are shown in Figure 4-10. In the left-hand example, a clear Cs-137-flux peak occurs at approximately 295 degrees azimuth. In the right-hand example, a faint U-238-flux peak occurs at approximately 68 degrees azimuth. As these examples show, the distinctness of azimuthal peaks can vary significantly. The precise azimuth of peaks is also uncertain owing to the asymmetry of the flux variation and the coarse measurement interval (22.5 degrees). Table 4-5 lists interpreted azimuthal peaks for the logs covered by this summary. The nuclides causing the azimuthal peaks and the quality of the peak are indicated, along with the interpreted azimuth direction. Where azimuthal peaks are observed to span several adjacent logging depths, the azimuth is interpreted from the depth corresponding to the strongest gamma ray flux.

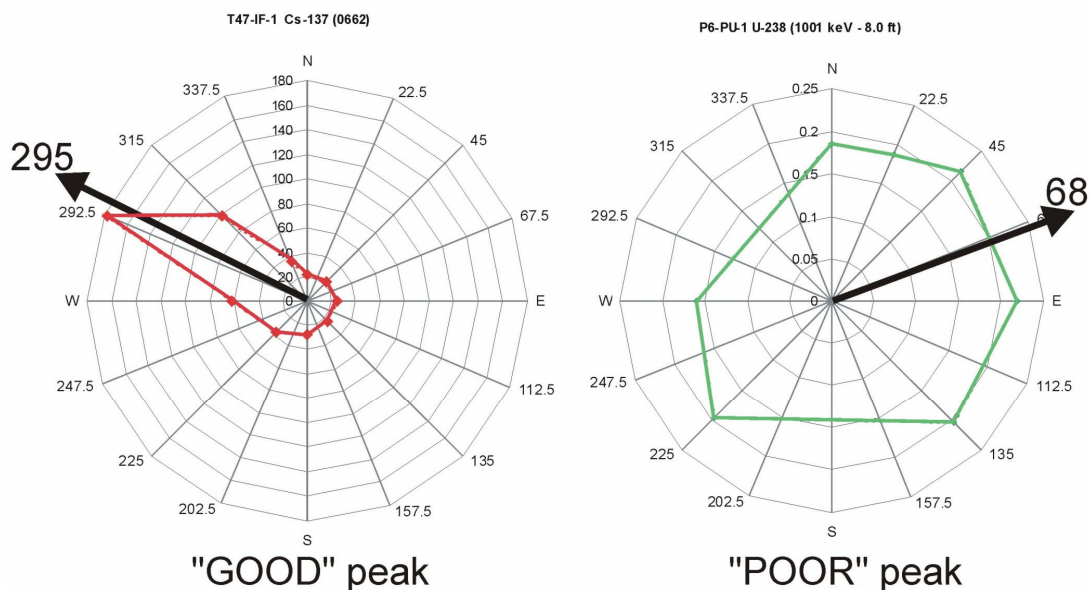


Figure 4-10. Azimuthal data plots showing examples of a highly directional gamma ray flux (left) and marginally directional gamma ray flux (right).

Table 4-5. Azimuthal logging data results summary.

| Probe_ID | Depth (ft bgs) | Azimuth (degrees) | Nuclide | Peak Quality |
|----------|-------------------|----------------------|--------------|--------------|
| T3-EU-02 | 8.0 | 169 | U-238 | Fair |
| T3-EU-03 | 8.0 | None | U-238 | Poor |
| T47-IF-1 | 8.0 | 290 | Cs, minor Co | Good |
| T47-IF-2 | 8.0 | 290 | Cs, minor Co | Good |
| T47-IF-2 | 10.0 | 124 | Cs, minor Co | Good |
| HAL2 | 12.0 | 191 | Cs, minor Co | Good |
| HAL2 | 21.0 | 90 | Cs, minor Co | Fair |
| HAL4 | 12.0 | 90 | Cs, Co | Fair |
| P5-UEU-1 | 9.0 | 280 | Pu | Good |
| P5-UEU-1 | 14.5 | 45 | Pu | Fair |
| P5-UEU-4 | 9.0 | 11 | Pu, Am | Good |
| P5-UEU-4 | 10.0 | 90 | Pu, Am | Good |
| P5-UEU-4 | 12.0 | 0 | Am | Poor |
| P5-UEU-4 | 14.0 | 135 | U-238 | Poor |
| P5-UEU-5 | 12.0 | 236 | Pu, Am, Np | Fair |
| P5-UEU-7 | 11.0 | 68 | Pu | Fair |
| P6-PU-1 | 8.0 | 34 | Am, Np, Pu | Good |
| P6-PU-1 | 8.0 | 68 | U-238 | Poor |
| P6-PU-1 | 10.0 | 90 | Pu | Fair |
| P6-PU-2 | 10.0 | 168 | Am | Fair |
| P6-PU-2 | 10.0 | 338 | Am | Poor |
| P6-PU-2 | 13.0 | 260 | Pu | Fair |
| P6-PU-3 | 7.74 | 185 | Pu, Np | Good |

The shape of azimuthal peaks, even for ideal point sources, varies for different radionuclides depending on gamma ray energy. This variation is because some gamma rays will always penetrate through the azimuthal shield, even when the shield's window is pointed directly away from the radionuclide source. Backside gamma ray penetration is greater for high-energy gamma rays (e.g., U-238 1,001 keV) than for lower-energy gamma rays (e.g., Pu-239 375 keV). Thus azimuthal peaks tend to be more subdued for the higher energy radionuclides. Azimuthal results should be corrected for this effect if it becomes important to make comparisons between the distribution of different radionuclides.

4.6.1 Subsurface Waste Heterogeneity as Observed from Azimuthal Logging Data

Azimuthal logs were collected at 0.5-ft intervals from 8.0–16.0 ft in Probehole P5-UEU-1. These logs provide some useful insight into the heterogeneity of the SDA subsurface. Probe P5-UEU-1 azimuthal plots for total gamma ray flux are presented in Figure 4-11. Homogenous conditions would be indicated by constant gamma ray flux in all azimuthal directions (i.e., roughly circular plots). Figure 4-11 shows that approximate homogenous conditions occur at a few depths, but most depths indicate heterogeneous conditions. Heterogeneity may be caused by nonuniform radionuclide distribution or nonuniform density distribution in the vicinity in the probehole. Probehole P5-UEU-1 data also show that the location and character of the heterogeneity changes gradually with depth.

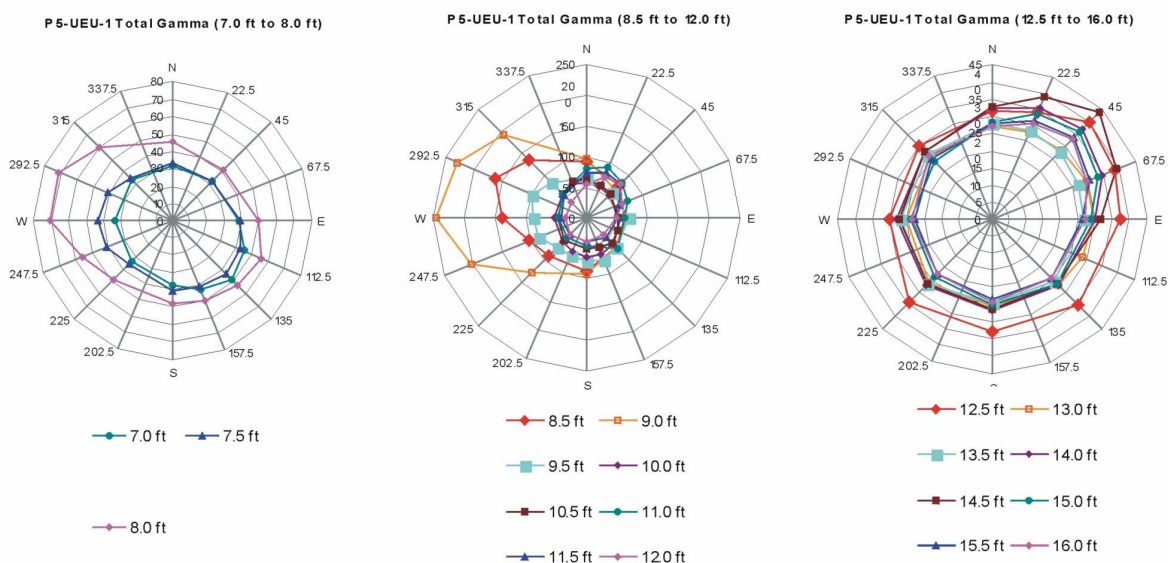


Figure 4-11. Azimuthal plots for total gamma ray flux in Probe P5-UEU-1.

4.7 Geophysics Database Compilation

During FY 2004, the probing project completed a compilation of surface and borehole geophysical data into the comprehensive Nuclear Logging and Surface Geophysics Database. Information about the structure, use, and maintenance of this data base may be found in PLN-1709.

The PLN-1709 provides documentation for the Nuclear Logging and Surface Geophysics Database, including software documentation, resource descriptions, and assumptions. The data-flow analysis, the logical software design, the physical system design, and data access module design documents are included as sections in this document.

4.8 Beryllium Block Investigation

The Early Actions Beryllium Block Encapsulation Project encapsulated buried beryllium reflector blocks and related reactor components within an injected grout material. Grout injection is accomplished via an injection well array that is installed surrounding the targeted beryllium block disposal site. Grout is injected throughout the depth interval containing the target shipment. Thus, the horizontal and vertical location of the beryllium block disposals is a prerequisite for engineering design of the grout injection system.

The “Determination of Beryllium Block Disposal Locations for the OU 7-13/14 Early Actions Beryllium Encapsulation Project” (EDF-4899), discusses the combined use of waste disposal inventory records, surface geophysical data, and tritium gas surveys to estimate the horizontal and vertical location of disposed beryllium blocks in the SDA. Beryllium disposals were evaluated in Trench 52, Trench 54, Trench 57, Trench 58, and Soil Vault Row 17.

4.9 Volatile Organic Compound Analysis using n-Gamma Logging Data

During FY 2004, the probing project completed an evaluation of methods for estimating VOC mass remaining within the SDA. Details of this investigation may be found Sondrup et al. (2004). A summary of the report findings is discussed below.

The purpose of the Sondrup et al. (2004) study was to provide an estimate of the mass fraction of carbon tetrachloride and VOCs remaining in the waste disposal pits at the SDA. Both OU 7-08 and 7-13/14 could use this information for estimating risk and making remediation decisions. The estimate initially was based on a comparison of the mass of VOCs originally buried at select locations in the SDA to the mass that currently remains at the same location, which is based on neutron-gamma logging of probeholes. However, a defensible estimate was not possible because of the inability to quantify uncertainty around the original estimate of chlorine mass per probehole and the inadequacy of the neutron-gamma logging-tool calibration function.

A revised strategy that also relied on neutron-gamma logging data was also unsuccessful because of (1) the inability to distinguish Series 743 sludge from other media (e.g., soil and debris) and (2) the inability to develop a tool-response function capable of predicting all observed neutron-gamma data. In addition, even if an adequate tool-response function were developed, it would remain difficult to defensibly estimate the mass of VOCs remaining in SDA pits without the ability to independently characterize both the matrix composition and the distribution of the chlorine-containing material around the neutron-gamma tool.

A simpler, alternative approach was used to approximate the amount of VOC mass remaining without any attempt to quantify the uncertainty. Based on the approach, an estimate of 50 percent VOC mass remaining is recommended as a starting point for numerical modeling to predict risk and remediation goals for OU 7-08 and OU 7-13/14. An estimate of 75 percent mass remaining is recommended as an upper bound. The lack of uncertainty surrounding these estimates should be carefully considered when interpreting any results derived from their use.

Because more precise estimates will almost certainly involve nuclear logging data, any further attempts to estimate the fraction of remaining mass should involve redesigning the neutron-gamma tool or performing a comprehensive calibration to conditions and materials that are more likely to be encountered in the waste pits. A broad-based, technically defensible strategy should be developed to logically ensure

the objectives of the project could be achieved. This strategy would likely involve redesigning the neutron-gamma tool so that it would (1) interrogate a volume of material that more closely approximates homogeneous conditions and (2) maximize sensitivity of the tool in the region of interest to the project (50 wt% chlorine in this case). It also should include a recalibration of the tool to constituents, other than chlorine, that are unique to Series 743 waste or be able, by some other means, to distinguish between Series 743 sludge and other media. In addition, the tool also will require a thorough calibration to conditions and materials that are more likely to be encountered in the waste pits or, alternatively, a model-based tool response developed for the same conditions and materials.

5. REFERENCES

- ASTM-D2216-98, 1998, "Standard Test Method for Laboratory Determination of Water (Moisture) Content of Soil and Rock by Mass," ASTM International.
- Beitel, G. A., P. Kuan, C. W. Bishop, and N. E. Josten, 2000, *Evaluation of OU 7-10 Stage I Soil Moisture Readings*, INEEL/EXT-00-00651, Rev. 0, Idaho National Laboratory.
- EDF-4899, 2004, "Determination of Beryllium Block Disposal Locations for the OU 7-13/14 Early Actions Beryllium Encapsulation Project," Rev. 1, Idaho Completion Project.
- GE, 1989, *Chart of the Nuclides*, 14th edition, General Electric Company.
- Giles, John R., Nick Josten, and Barbara J. Broomfield, 2003, *Evaluation of Nuclear Logging Tool Calibrations for use in Type A Probes at the INEEL Subsurface Disposal Area, OU 7-13/14*, INEEL/EXT-03-00118, Rev. 0, Idaho National Laboratory.
- Holdren, K. Jean, Bruce H. Becker, Nancy L. Hampton, L. Don Koeppen, Swen O. Magnuson, T. J. Meyer, Gail L. Olson, and A. Jeffrey Sondrup, 2002, *Ancillary Basis for Risk Analysis of the Subsurface Disposal Area*, INEEL/EXT-02-01125, Rev. 0, Idaho National Laboratory.
- INL, 2002, *Type A Nuclear Logging Data Acquisition and Processing for Operable Units 7- 13/14 and 7-10*, INEEL/EXT-02-00558, Rev. 1, Idaho National Laboratory.
- Jewell, James K., L. Reber Edward, and C. Hertzog Russell, 2002, *Estimating the Mass of Pu-239 Waste Near P9-20 Probe Hole for the OU 7-10 Glovebox Excavator Method Project*, INEEL/EXT-02-01189, Rev. 0, Idaho National Laboratory.
- Josten, N. E. and J. C. Okeson, 2000, *OU 7-10 Initial Probing Campaign Downhole Logging Results*, INEEL/EXT-2000-00526, EDF-ER-207, Rev., Idaho National Laboratory.
- Josten, Nicholas E., 2002, *Compilation of Analytical Notes and Data Analyses for the Integrated Probing Project 1999-2002*, INEEL/EXT-02-01306, Rev. 0, Idaho National Laboratory.
- McElroy, D. L. and J. M. Hubbell, 1990, *Hydrologic and Physical Properties of Sediments at the Radioactive Waste Management Complex*, EGG-BG-9147, Idaho National Laboratory.
- PLN-1709, 2004, "Software Documentation for the Nuclear Logging and Surface Geophysics Database," Rev. 0, Idaho Completion Project.
- SOW-561, 2003, "Statement of Work for Nuclear Geophysical Logging," Rev. 0, Idaho National Laboratory.
- Sondrup, A. Jeffrey, Eric C. Miller, Edward H. Seabury, and Nick Josten, 2004, *Estimating Carbon Tetrachloride and Total Volatile Organic Compound Mass Remaining in Subsurface Disposal Area Pits*, ICP/EXT-04-00396, Idaho Completion Project.

